Influence of internal disorder on the superconducting state in the organic layered superconductor κ-(BEDT-TTF)$_2$Cu[N(CN)$_2$]Br

M. Pinterić*

*Institute of Physics, P. O. Box 304, HR-10001 Zagreb, Croatia
and Faculty of Civil Engineering, University of Maribor, SLO-2000 Maribor, Slovenia*

S. Tomić, M. Prester, and Đ. Drobac

Institute of Physics, P. O. Box 304, HR-10001 Zagreb, Croatia

K. Maki

*Max-Planck Institute for the Physics of the Complex Systems, D-01187 Dresden, Germany
and Department of Physics and Astronomy, University of Southern California, Los Angeles, California 90089-0484*

We report high-sensitivity ac susceptibility measurements of the penetration depth in the Meissner state of the layered organic superconductor κ-(BEDT-TTF)$_2$Cu[N(CN)$_2$]Br. We have studied nominally pure single crystals from the two different syntheses and employed controlled cooling procedures in order to minimize intrinsic remnant disorder at low temperatures associated with the glass transition, caused by ordering of the ethylene moieties in BEDT-TTF molecule at $T_G = 75$ K. We find that the optimal cooling procedures (slow cooling of -0.2 K/h or annealing for 3 days in the region of T_G) needed to establish the ground state depend critically on the sample origin, indicating different relaxation times of terminal ethylene groups. We show that, in the ground state, the behavior observed for nominally pure single crystals from both syntheses is consistent with unconventional d-wave order parameter. The in-plane penetration depth $\lambda_{\text{in}}(T)$ is strongly linear, whereas the out-of-plane component $\lambda_{\text{out}}(T)$ varies as T^2. In contrast, the behavior of single crystals with long relaxation times observed after slow (-0.2 K/h) cooling is as expected for a d-wave superconductor with impurities [i.e., $\lambda_{\text{in}}(T) \propto \lambda_{\text{out}}(T) \propto T^2$] or might be also reasonably well described by the s-wave model. Our results might reconcile the contradictory findings previously reported by different authors.

I. INTRODUCTION

Since the discovery of superconductivity in κ-BEDT-TTF-based materials a decade ago,[1,2] the question of pairing symmetry has remained as one of the most intriguing issues. From the very beginning, these materials have attracted a lot of interest, not only because they achieved the highest superconducting (SC) transition temperatures (T_C) among organic materials, but also because of their similarities to the high-temperature cuprate superconductors. First, the κ-(BEDT-TTF)$_2 X$ [abbreviated as κ-(ET)$_2 X$] are strongly anisotropic, quasi-two-dimensional materials, with a very weak interplane coupling. This feature is due to the crystalographic structure, in which orthogonally aligned BEDT-TTF dimers form two-dimensional (2D) conducting layers sandwiched between the polymerized anion (X) layers. Second, antiferromagnetic (AF) and SC phases occur next to one another, which suggests that electron correlations play significant role in the establishment of the ground state. Indeed, the ground state of κ-(BEDT-TTF)$_2$Cu[N(CN)$_2$]Cl material is an insulating AF phase with mildly canted spins,[4,3] while the ground state of κ-(BEDT-TTF)$_2$Cu[N(CN)$_2$]Br [abbreviated as κ-(ET)$_2$Br] and κ-(BEDT-TTF)$_2$Cu(NCS)$_2$ [abbreviated as κ-(ET)$_2$NCS] is a SC phase. In the former, the applied pressure suppresses the AF state and stabilizes the SC state,[5] whereas by deuterization of κ-(ET)$_2$Br, the ground state is

gradually pushed from the SC toward the AF state.[6] The phase diagram is, therefore, quite similar to that of the cuprates if doping is replaced by pressure or deuterization. Third, the normal state has some properties that are distinct from conventional metals, supporting the importance of electron correlations. In particular, the Knight shift decreases significantly below about 50 K, suggesting a suppression of the density of states—that is, the appearance of a pseudogap near the Fermi energy.[7] A broad dip in the electronic density of states around the Fermi energy was also observed by scanning tunneling microscopy (STM) measurements below about the same temperature.[8] Further, there is a peak in $1/T_1 T$ at about 50 K, where T_1 is the nuclear spin-lattice relaxation time, which suggests the presence of short-range AF correlations.[7] This peak disappears under pressure concomitantly with superconductivity.

The presence of significant electron correlations strongly favors the possibility of an unconventional SC. Results in favor of a d-wave order parameter have been obtained by different experimental techniques. ^{13}C NMR measurements showed that the spin-lattice relaxation rate follows a T^3 dependence at very low temperatures. This result, together with the Knight shift experiment, provides evidence for spin-singlet pairing with nodes in the gap.[9] The low-temperature specific heat,[10] as well as the thermal conductivity,[11] also showed a power-law behavior $c_s(T) \propto T^2$ and $\kappa(T) \propto T$, respectively. Further, the magnetic penetration depth $\lambda(T)$,

measured by microwave cavity perturbation,[12] muon-spin relaxation,[13] tunnel diode oscillation,[14] and ac susceptibility,[15,16] also displayed the power-law behavior, usually in the form of a T and/or a T^2 behavior for $\lambda(T)$ at low temperatures.

Recent angle-resolved measurements of the SC gap structure using STM (Ref. 17) and thermal conductivity[18] clearly showed fourfold symmetry in the angular variation characteristic of the d-wave superconducting gap. Both measurements have revealed that nodes are directed along directions rotated by 45° relative to the in-plane crystal axes, indicating $d_{x^2-y^2}$-wave superconductivity. Such a nodal structure indicates that both Fermi surfaces (oval-shape quasi-two-dimensional hole cylinder band and an open quasi-one-dimensional band[19]) should participate in SC pairing in contrast with theoretical predictions of superconductivity induced by AF spin fluctuations.[20]

In contrast, some other penetration depth studies,[21–23] as well as the most recent specific heat measurements,[24,25] led to results favoring a conventional s-wave order parameter. In particular, a strong-coupling s-wave order parameter was claimed to be observed in the latter experiments.

The question arises as to what the source of the conflicting results is and how this discrepancy could be resolved. As far as experimental determination of $\lambda(T)$ in the mixed state is concerned, the complex vortex dynamics might present a serious problem already at fields as low as 70–300 Oe, as pointed out by Lee *et al.*[26] Further, additional complications might be due to an order-disorder transition that bears glassy features, taking place at $T_G \approx 75$ K for κ-(ET)$_2$Br or at $T_{G1} \approx 70$ K and $T_{G2} \approx 53$ K for κ-(ET)$_2$NCS.[27,28] The transition region is situated between 65 and 85 K and between 45 and 75 K for κ-(ET)$_2$Br and κ-(ET)$_2$NCS systems, respectively. The transition is ascribed to the gradual freezing down of the remaining motion of the ethylene groups of the BEDT-TTF molecules that are thermally activated at high temperatures between the two possible conformations. That is, the relative orientation of the outer C-C bonds can be either eclipsed or staggered. Upon lowering the temperature, the former and latter are adopted for κ-(ET)$_2$Br and κ-(ET)$_2$NCS, respectively. X-ray diffraction measurements showed that at 125 K (CH$_2$)$_2$ groups are ordered in average in the whole bulk.[29] However, the passage through the region of glassy transition appears to play a crucial role regarding the level of residual intrinsic disorder at low temperatures. This might be also due to the anomalous changes in thermal expansion behavior inside the same temperature region.[30,31] Rapid cooling rates are reflected in the smaller resistivity ratio between T_G and T_C and larger resistivity humps centered at about 60 K.[6,32] The understanding of the transport properties in the normal state is further complicated by the fact that the standard resistivity behavior that resembles a semiconducting state above 100 K,[33] whereas it becomes metallic below, is not reported for all syntheses.[34] In the latter case, samples display a metallic behavior in the whole temperature range between room temperature (RT) and T_C. In addition, indications are given that some Cu(II) may replace regular Cu(I) during synthesis, affecting the resistivity behavior.[35] The correlation between different mean free paths in samples of different syntheses

and the presence of Cu(II) ions was also suggested.[36] Further, sample dependence and relaxation effects were also observed in the magnetization measurement results for κ-(ET)$_2$Br.[37] Samples of one synthesis show two peaks in the magnetization versus field (M-H) curve, in contrast to crystals of another synthesis that show only one. Finally, the observed anomalous cooling rate dependence of the M-H curve was attributed to the change in the resistivity curves and remnant disorder in the sample.

In an attempt to reconcile the existing contradictions and determine the pairing symmetry of the genuine SC ground state, we have undertaken an investigation that covered a broad range of single crystals of various syntheses and in which the influence of thermal cycling and sample history was checked in carefully designed experiments. We have performed a high-resolution ac susceptibility measurements in the Meissner state in the two field geometries, i.e., when ac field was parallel and perpendicular to the crystal planes. A quantitative data analysis, which we have elaborated with scrutiny to account for the demagnetization correction in the latter geometry, enabled us to get a full characterization of each sample under study, clarifying in this way a previously suspected sample dependence. Indeed, our experiments show that cooling procedures in the region of the glass transition, necessary to establish the bulk SC ground state, critically depend on the sample origin. In particular, our results demonstrate that the low-temperature state is critically determined by the time scale of the experiment in the region of the glass transition, revealing in that way different relaxation times of terminal ethylene groups in samples from two distinct syntheses studied in the most detail. We show that in the ground state, the behavior observed for nominally pure single crystals from both syntheses is consistent with an unconventional d-wave order parameter; that is, the low-temperature in-plane and out-of-plane superfluid densities are proportional to T and T^2, respectively. However, the behavior of the superfluid density observed after standard a slow cooling for single crystals with long relaxation times deviates from that found in the ground state. It is as expected for a d-wave superconductor with impurities or might be reasonably well described by the s-wave model. These results may give a solution to a decade long mystery with regard to the symmetry pairing in κ-BEDT-TTF superconductors. A preliminary report was given in Ref. 38.

II. EXPERIMENTAL TECHNIQUE

Measurements of the complex ac susceptibility ($\chi = \chi' + i\chi''$) were performed using a commercial ac susceptometer (CryoBIND/Sistemprojekt, Zagreb). The sensitivity of the system, expressed in equivalent magnetic moments, was $\Delta m = 2 \times 10^{-9}$ emu in the broad temperature range between 1.5 K and T_C.[39] Measurements were performed with $H_{ac} = 14$ mOe at $f = 231$ Hz. A gold 0.07% iron-copper thermocouple was used as a thermometer. The sample was placed in the upper one of two identical secondary coils immersed in a liquid helium bath, positioned in such a way that the applied ac field was either perpendicular or parallel to the conducting planes of the single crystals under study. In the remainder of
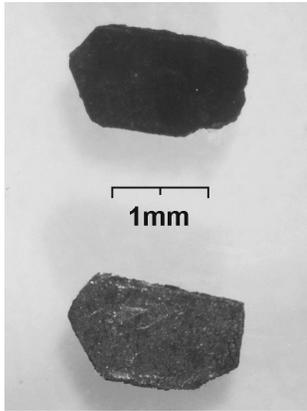
FIG. 1. The κ-(ET)$_2$Br (above) and its reference sample (below).

the paper, the case of a magnetic field aligned with the b crystallographic axis, i.e., perpendicular to the high-conducting ac crystallographic planes, is denoted by $H_{ac}\perp$ plane, while the case of a magnetic field direction lying inside the ac crystallographic plane is denoted by $H_{ac}\parallel$ plane. In order to probe the sample in the Meissner state care was taken to reduce the amplitude of the ac field (H_{ac}) until the component $\chi'(T)$ was independent of H_{ac} ($H_{ac}<42$ mOe) and the $\chi''(T)$ component was negligible. No frequency dependence (13 Hz$<f<$2 kHz) was observed for H_{ac} <1 Oe. In addition no influence of the Earth's field was observed: runs performed with compensation for the Earth's field gave the same results. This is in accordance with the fact that the reported values for lower critical magnetic fields $H_{C1}(T)$, corrected for demagnetization, are far above the Earth's field H_E for all temperatures below 8 K. In this temperature range $H_{C1}(T)\geq 10$ Oe,[40] while the value of the Earth's field determined in our laboratory is $H_E\approx 0.36$ Oe.[41]

The calibration of the system was performed with a piece of specially and carefully designed niobium foil, which we will refer to, in the remainder of the paper, as the reference sample. For each κ-(ET)$_2$Br single crystal, a special reference sample was created independently to ensure that its dimensions and shape were as close as possible to the original (see Fig. 1). We start with the conventional formula, which relates the induced voltage on the detection coil U, the measured susceptibility χ'_m, the demagnetization factor D, the volume V, and the internal susceptibility χ'; that is, χ'_m corrected for the demagnetization effect $1/(1+D\chi')$:

$$U \propto V\chi'_m = V\frac{\chi'}{1+D\chi'}. \tag{1}$$

Here we have taken into account that measured samples are much smaller than the detection coil. If we use a conventional calibration assumption that the susceptibility for niobium reference sample at low temperatures can be taken to be -1, we can finally determine the internal value of the susceptibility according to formula

$$\chi' = -\frac{V_r}{V}\frac{\dfrac{1}{1-D_r}}{\dfrac{1}{1+D\chi'}}\frac{U}{U_r}, \tag{2}$$

where the index "r" designates the reference sample. When the ac field was parallel to the crystal planes, the demagnetization effect could be neglected, meaning that the middle factor in Eq. (2) can be simply replaced by unity. In order to correct the measured data for the demagnetization factor for the ac field perpendicular to the crystal planes, we have developed a method which strongly reduces the experimental error in χ' to less than 1% and allows us to get a reliable absolute value of the penetrated volume $1+\chi'$ for this geometry, as well. The latter quantity directly determines the penetration depth and the superfluid density, as we show in Secs. III B and III C. In the following, we argue and show that our claim is justified.

Our starting point is that the reference sample represents a perfect copy of the sample under study (Fig. 1), implying very close values of the respective demagnetization factors D and D_r. Since the κ-(ET)$_2$Br sample is almost completely diamagnetic in this geometry, we can use the approximation $\chi'\approx -1$. Therefore, demagnetization effects for both samples must be very close in value and the middle factor in Eq. (2) in the first order of approximation can be replaced by unity. Further, in order to improve the precision and eliminate a small remaining difference in the demagnetization effect, the middle factor in the second order of approximation is calculated by the following procedure. Both κ-(ET)$_2$Br and the reference sample were taken to be fully superconducting disks (that is, thin cylinders with an aspect ratio of length and diameter of about 0.4) with the same face area and the same thickness as their originals. We consider the disk approximation to be more suitable for a description of the real sample than the elipsoid one, used by authors of Ref. 6. We base this assertion on the fact that the former approximation better describes rather sharp sample edges, which might give a substantial contribution to the demagnetization factor. The middle factor in Eq. (2) is then given by the calculated ratio of diamagnetic effects for these two bodies,

$$\frac{1}{1-D_{disk,r}}\bigg/\frac{1}{1-D_{disk}}.$$

The systematic error due to the approximation of the specific shape of samples to the shape of the disk obviously cancels out by division. Numerical data for the demagnetization factor for the disk were taken from the literature.[42]

In order to calculate the area and thickness, the dimensions of both κ-(ET)$_2$Br and the reference sample were carefully measured with a high precision of 1%. The precision was verified by the following procedure. All significant niobium reference sample dimensions were measured and the volume calculated. In addition, the same reference sample was weighted and the volume calculated using the niobium density $\rho_{Nb}=8.57$ g/cm^3. The difference between two obtained values was always about 1%. Finally, the middle fac-
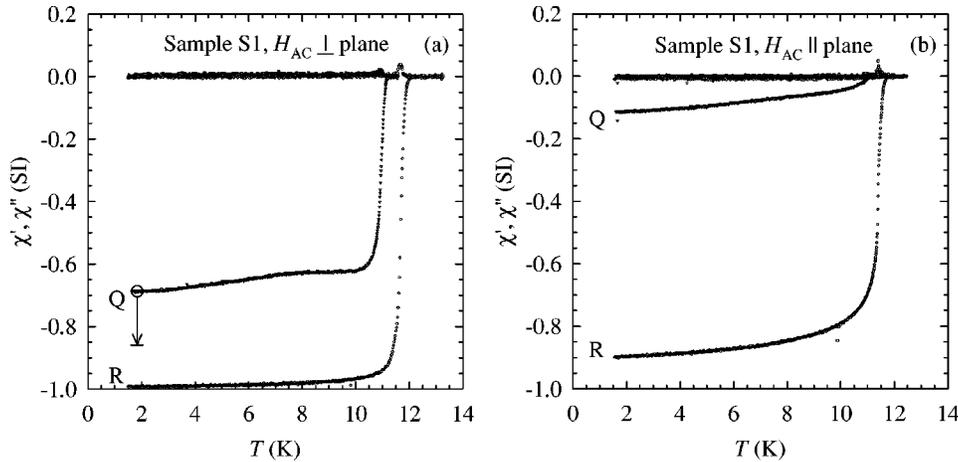
FIG. 2. Sample S1: real and imaginary parts of the susceptibility for relaxed (R) and quenched (Q) states in (a) $H_{ac}\perp$ plane and (b) $H_{ac}\|$ plane geometry. The arrow in (a) illustrate the upper limit of the systematic error.

tor in Eq. (2) obtained in this way differs from unity only for a few percent. This shows that the calculation procedure and the starting assumption are valid.

In the end, we estimate that our calibration procedure for $H_{ac}\perp$ plane is accurate in $1+\chi'$ to 33% for χ' close to -1 and to about 50% for $-0.96 > \chi' > -0.5$. As for the $H_{ac}\|$ plane, the accuracy in $1+\chi'$ is estimated to be about 15% for all measured low-temperature χ' values.

Nominally pure single crystals of κ-$(ET)_2Br$, originating from two different syntheses had different resistivity ratios $RR(75 \text{ K}/T_{min})$ for similar cooling rates employed.[34,43] $RR(75 \text{ K}/T_{min}) = \rho(75 \text{ K})/\rho_{min}$, where ρ_{min} is the resistivity measured at temperature just above the SC transition. Single crystals with $RR(75 \text{ K}/T_{min}) \approx 200$ and ≈ 50 obtained by standard slow cooling rate have been labeled as S1 and S2, respectively.

Three different cooling procedures were used to cool samples from RT to 4.2 K. Special care was taken in the temperature range 60 K$<T<$100 K, where relaxation processes appear.[27,28] For the *quenched* (denoted as Q) state the sample was cooled down to liquid helium temperature in about 1 min, which represents an average speed of about -300 K/min. over the whole temperature range. For the *relaxed* (denoted as R) state the sample was first cooled to 100 K in about 10 min. Between 60 K and 100 K the cooling rate was carefully monitored to amount to about -0.2 K/min.

Below 60 K, the sample was finally cooled to 4.2 K in a few minutes. For the *annealed* state (denoted as A) the sample was cooled down to liquid nitrogen temperatures in about 1 h. Then it was kept between liquid nitrogen temperature and 100 K for three days. Finally, it was cooled down to liquid helium temperature in a few minutes. The samples used in this study were rhombic platelets with face areas between 0.51 and 2.15 mm^2 and thickness between 0.29 and 0.70 mm.

III. RESULTS AND ANALYSIS

A. Complex susceptibility

Our first important result concerns the influence of the cooling rate on the components of the complex susceptibility in the SC state as a function of the synthesis procedure. We present the behavior obtained in two principal field geometries: that is, $H_{ac}\perp$ plane and $H_{ac}\|$ plane, as defined in Sec. II. On the basis of our previous measurements with the magnetic field aligned with the a and c crystallographic axes,[15] we know that the specific orientation within the ac crystallographic plane does not influence the obtained result for the penetration depth since the out-of-plane component is a dominant contribution. Therefore, we always made sure that the field was aligned with the largest dimension of the platelet face in order to minimize the demagnetization factor.
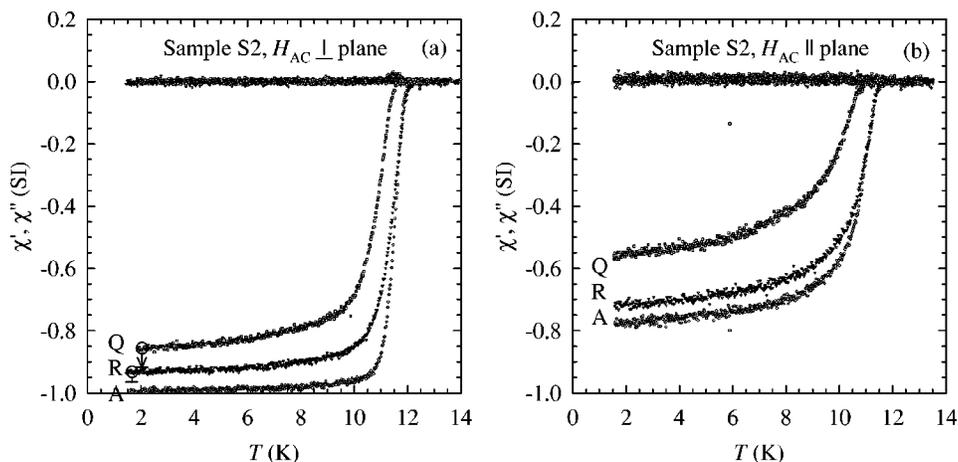
FIG. 3. Sample S2: real and imaginary parts of the susceptibility for annealed (A), relaxed (R), and quenched (Q) states in (a) $H_{ac}\perp$ plane and (b) $H_{ac}\|$ plane geometry. The arrows in (a) illustrate the upper limit of the systematic error.
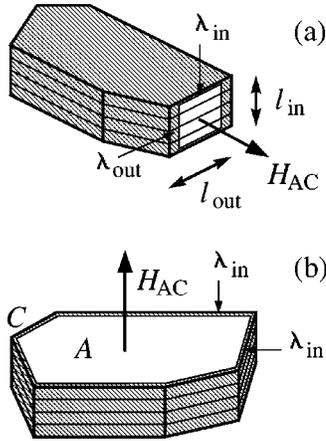
FIG. 4. Simplified depiction of the sample in the magnetic field (a) $H_{ac}\parallel$ plane and (b) $H_{ac}\perp$ planes. Shaded parts of the sample represent the volume penetrated by the magnetic field. Condition $\lambda_{out}/\lambda_{in} \gg l_{in}/l_{out}$ in (a) ensures that λ_{in} can be neglected in the analysis (Ref. 15).

Susceptibility data obtained for sample S1 for two different cooling rates are shown in Fig. 2. We identify the R state as the *ground state*. In the ground state, superconductivity sets in at 12.0 K and 11.5 K for $H_{ac}\perp$ plane and $H_{ac}\parallel$ plane, respectively. We have already reported the difference in T_C, as the well as anisotropy in the susceptibility for H_{ac} perpendicular and parallel to the planes.[15] Here we report, to the best of our knowledge for the first time, the absolute susceptibility values in both field geometries. For $H_{ac}\perp$ plane the sample response is almost completely diamagnetic, while for $H_{ac}\parallel$ plane the susceptibility is somewhat smaller in magnitude. Next, our new result points to a huge effect of the cooling rate on the susceptibility value and T_C. When the sample was cooled faster, the absolute value of the susceptibility was smaller and T_C lower. In other words, the diamagnetic region shrinks in the χ' vs T plot. This huge effect is especially emphasized for $H_{ac}\parallel$ plane geometry, where the absolute χ' value is almost an order of magnitude smaller for the Q state than for the R state.

Susceptibility data obtained for sample S2 for three different cooling rates are presented in Fig. 3. The first feature, reflecting a different sample quality, is that the ground state,

characterized as before by an almost complete diamagnetic response, is established in the A state, and not, as in the case of sample S1, in the R state. For the purpose of clarity, we will refer to the R state of sample S2 as the *intermediate state*.[56] The anisotropy of the susceptibility in the ground state is somewhat larger for sample S2 than for sample S1. The second feature is in that the cooling rate effect on the susceptibility value is much smaller for sample S2 compared with the effects obtained for sample S1 (see Fig. 2).

Finally, we point out that the $\chi''(T)$ component was negligible, indicating clearly that the measured samples were in the Meissner state.

B. Penetration depth

Further, we analyze the susceptibility data for the hereabove described single crystals of different quality in order to get the penetration depth temperature behavior and the values at zero temperature. In $H_{ac}\parallel$ plane geometry we have already argued that the in-plane penetration depth λ_{in} can be neglected in the analysis and that the out-of-plane penetration depth λ_{out} can be obtained from the susceptibility data using the formula for a thin superconducting plate in a parallel field[15] [see Fig. 4(a)]:

$$1 + \chi' = \frac{2\lambda_{out}}{l_{out}}\tanh\left(\frac{l_{out}}{2\lambda_{out}}\right). \quad (3)$$

Now we address in more detail the $H_{ac}\perp$ plane geometry. The magnetic field is strictly perpendicular to the conducting planes, so is the responding magnetization that expels it out of the bulk. The resultant circulating supercurrents will therefore flow within planes, which will only give a contribution to λ_{in} [see Fig. 4(b)]. In order to obtain an appropriate formula for the analysis, we start with the generalization of Eq. (3). We take into account that the ratio between the doubled penetration depth $2\lambda_{out}$ and the sample width in the direction of field penetration l_{out} is the ratio between the volume penetrated by the magnetic field V_P and the whole sample volume V. Therefore,

$$1 + \chi' = \frac{V_P}{V}\tanh\frac{V}{V_P}. \quad (4)$$
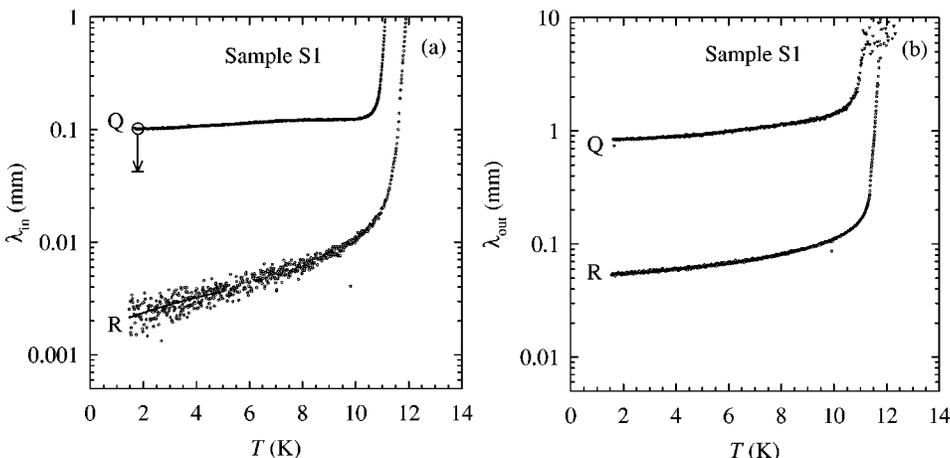
FIG. 5. Sample S1: (a) in-plane and (b) out-of-plane penetration depths for relaxed (R) and quenched (Q) states. Solid lines represent the fit to the power-law behavior, while the arrow in (a) illustrates the upper limit of the systematic error.
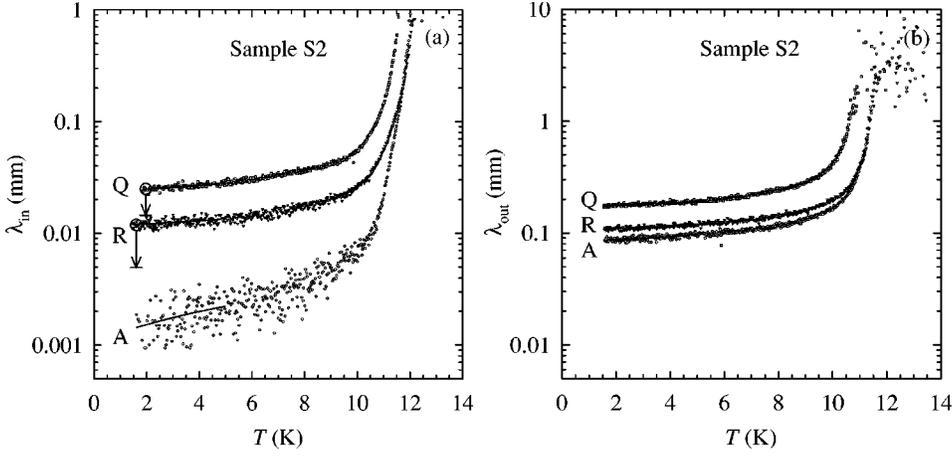
FIG. 6. Sample S2: (a) in-plane and (b) out-of-plane penetration depths for annealed (*A*), relaxed (*R*), and quenched (*Q*) states. Solid lines represent the fit to the power-law behavior, while the arrows in (a) illustrate the upper limit of the systematic error.

We note that, if the sample has the shape of a platelet, the magnetic field penetrates along the whole edge of the face. We can rewrite Eq. (4) as

$$1 + \chi' = \frac{C\lambda_{in}}{A} \tanh\frac{A}{C\lambda_{in}}, \qquad (5)$$

where C is the circumference, A the area of the platelet face, and λ_{in} the in-plane penetration depth [see Fig. 4(b)].

Our second important result concerns the temperature dependence of λ_{in} and λ_{out} in the ground state as a function of the synthesis procedure. In Figs. 5 and 6 we show the influence of the cooling rate on the anisotropic penetration depth as a function of the sample quality. Note that in the ground state of both samples S1 and S2 the temperature dependence of λ_{in} and λ_{out} at temperatures below about 5 K is well described by the T and T^2 law, respectively. The upper bound of the fit range (5 K) is given by the general requirement that the genuine low-temperature behavior of the penetration depth be strictly obeyed only far from the critical region close to T_C. The solid lines correspond to the calculated fit to the power-law behavior in the temperature range 1.6 K $< T <$ 5 K:

$$\lambda_{in} = k_{in}\left(\frac{T}{T_C}\right) + \lambda_{in}(0), \qquad (6)$$

$$\lambda_{out} = k_{out}\left(\frac{T}{T_C}\right)^2 + \lambda_{out}(0). \qquad (7)$$

We get $k_{in} = 5.2~\mu$m, $\lambda_{in}(0) = 1.5 \pm 0.5~\mu$m, $k_{out} = 56~\mu$m, $\lambda_{out}(0) = 53 \pm 10\mu$m and $k_{in} = 2.8~\mu$m, $\lambda_{in}(0) = 1.1 \pm 0.4\mu$m, $k_{out} = 69~\mu$m, $\lambda_{out}(0) = 85 \pm 10\mu$m for S1 and S2, respectively. The penetration depth values at 0 K, $\lambda(0)$, observed in the ground states of both samples, are in a very good accordance with values for the penetration depths given in the literature.[12,14,15,23,26,44–46]

Special attention should be given to the relative change of the penetration depth at low temperatures, $\eta(T) = [\lambda(T) - \lambda(0)]/\lambda(0)$. We denote the deviation of $\lambda_{in}(T)$ and $\lambda_{out}(T)$ from their values at 0 K, in units of $\lambda(0)$, as $\eta_{in}(T)$ and $\eta_{out}(T)$, respectively. We find that $\eta_{in}(5~\text{K}) = 1.4$, $\eta_{out}(5~\text{K}) = 0.19$ and $\eta_{in}(5~\text{K}) = 1.1$, $\eta_{out}(5~\text{K}) = 0.15$ in the

ground state of samples S1 and S2, respectively. First we note that η values are in perfect accordance for both samples, confirming that they are in the same—ground—state. Second, a difference between η_{in} and η_{out} values for almost an order of magnitude proves a strong anisotropy in physical properties between the two orientations. This also confirms our choice for the exponent in the power law in Eqs. (6) and (7).

Finally, our third important result concerns the intermediate state (*R* state in sample S2), for which we get $\eta_{in}(5~\text{K}) = 0.13$, $\eta_{out}(5~\text{K}) = 0.10$. Unlike for the ground state, the temperature dependences of λ_{in} and λ_{out} are so similar that they cannot be any longer described by different power laws as was the case in the ground state. The obvious solution is to try to fit both penetration depths to the T^2 power-law behavior

$$\lambda_{in} = k_{in}\left(\frac{T}{T_C}\right)^2 + \lambda_{in}(0), \qquad (8)$$

$$\lambda_{out} = k_{out}\left(\frac{T}{T_C}\right)^2 + \lambda_{out}(0), \qquad (9)$$

which suggests a *d*-wave superconductor with impurities. We get $k_{in} = 9.2~\mu$m, $\lambda_{in}(0) = 12 \pm 6~\mu$m, and $k_{out} = 58~\mu$m, $\lambda_{out}(0) = 110 \pm 20~\mu$m. We point out that the fit to the *s*-wave model describes our data almost equally well (see Sec. III C). On the other hand, the *s*-wave model fails completely for the penetration depth temperature dependences in the ground state of both samples S1 and S2.

Now we comment on the penetration depth results for the *Q* state. We find that $\eta_{in}(5~\text{K}) = 0.11$, $\eta_{out}(5~\text{K}) = 0.12$ and $\eta_{in}(5~\text{K}) = 0.16$, $\eta_{out}(5~\text{K}) = 0.10$ for samples S1 and S2, respectively. Here we apply the same arguments as in the case of the intermediate state and fit both λ_{in} and λ_{out} to the T^2 power-law behavior [Eqs. (8) and (9)]. We get $\lambda_{in}(0) = 100 \pm 50~\mu$m, $\lambda_{out}(0) = 830 \pm 100~\mu$m and $\lambda_{in}(0) = 24 \pm 12~\mu$m, $\lambda_{out}(0) = 170 \pm 20~\mu$m for sample S1 and S2, respectively. The fact that these fits describe the penetration depth data well again suggests a *d*-wave superconductor with impurities. Further, it should be noted that (i) $\lambda(0)$ values are larger for the *Q* state than for the intermediate state, suggesting a larger disorder in the former state, and (ii) $\lambda(0)$

TABLE I. Penetration depth properties, as defined in text, for (i) sample S1 in the relaxed (ground) and quenched states, and (ii) sample S2 in the annealed (ground), relaxed (intermediate), and quenched states.

State	$\lambda_{in}(0)$ (μm)	$\lambda_{out}(0)$ (μm)	k_{in} (μm)	k_{out} (μm)	η_{in}(5 K)	η_{out}(5 K)
			Sample S1			
R	1.5 ± 0.5	53 ± 10	5.2	56	1.4	0.19
Q	100 ± 50	830 ± 100	60	480	0.11	0.12
			Sample S2			
A	1.1 ± 0.4	85 ± 10	2.8	69	1.1	0.15
R	12 ± 6	110 ± 20	9.2	58	0.13	0.10
Q	24 ± 12	170 ± 20	22	88	0.16	0.10

values for sample S1 are significantly larger than ones for S2, suggesting significantly larger disorder in the former sample in the Q state. Finally, the result that $\lambda_{out}(0)$ for sample S1 is close to the crystal size indicates that the bulk superconductivity is not established, allowing us to define the boundary between bulk and nonbulk SC at $\chi' = -0.7$ for $H_{ac} \perp$ plane.

For clarity, all results for penetration depth properties presented in this Section are summarized in Table I.

C. Superfluid density

In the following, we address the temperature dependance of the superfluid density in order to get information on the symmetry of the superconducting state. We construct the in-plane superfluid density $\rho_{s,in}$ and out-of-plane superfluid density $\rho_{s,out}$ as

$$\rho_{s,in} = \left(\frac{\lambda_{in}(0)}{\lambda_{in}(T)} \right)^2, \tag{10}$$

$$\rho_{s,out} = \left(\frac{\lambda_{out}(0)}{\lambda_{out}(T)} \right)^2. \tag{11}$$
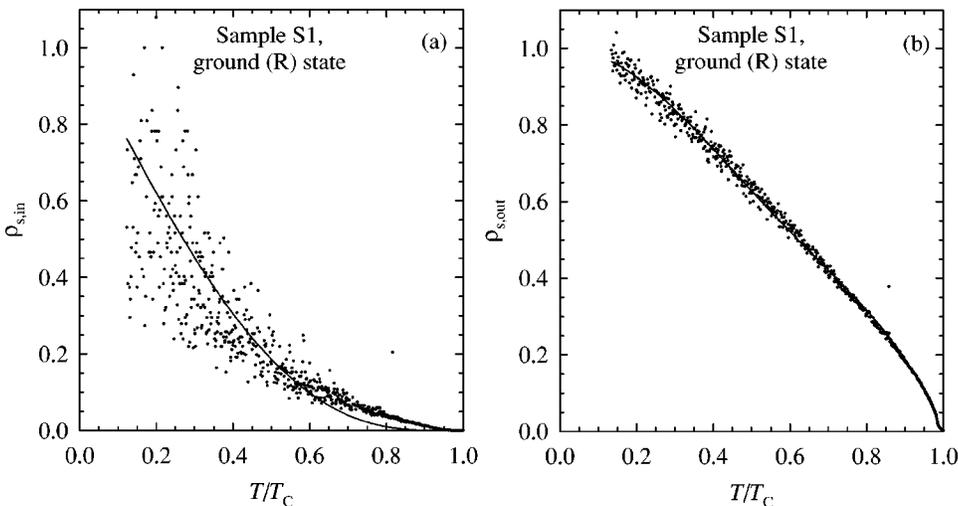
$\rho_{s,in}$ and $\rho_{s,out}$ for the ground state of sample S1 (established in the R state) and for the ground state of sample S2 (established in the A state) as a function of reduced temperature $t = T/T_C$ are displayed in Figs. 7 and 8, respectively. There is a strong resemblance in the behavior found for both samples. Note that the leading terms, which describe the low-temperature behavior, are the T and T^2 terms for $\rho_{s,in}$ and $\rho_{s,out}$, respectively.[15] This is to be expected, because T and T^2 terms describe the low-temperature behavior of the λ_{in} and λ_{out} in the ground state. If we expand the leading term to the full polynomial, in order to fit the superfluid density data in the whole temperature region below T_C, we finally obtain for sample S1

$$\rho_{s,in} = 1 - 1.95t + 1.45t^3 - 0.09t^4 - 0.41t^5, \tag{12}$$

$$\rho_{s,out} = 1 - 1.88t^2 - 0.73t^3 + 4.47t^4 - 2.86t^5, \tag{13}$$

and for sample S2

$$\rho_{s,in} = 1 - 1.68t + 0.78t^3 + 0.16t^4 - 0.26t^5, \tag{14}$$

$$\rho_{s,out} = 1 - 1.45t^2 + 2.98t^3 - 5.38t^4 + 2.84t^5. \tag{15}$$

Taking into account a relatively large experimental error in the penetration depth values (see Figs. 5 and 6), the leading coefficient values might be considered to be almost the same. In addition to the systematic error, there is also a noise, which is a mere consequence of the fact that $\rho_{s,in}$ is calculated according to the expression $\rho_{s,in}(T) = [\lambda_{in}(0)/\lambda_{in}(T)]^2$, so that the absolute noise in $\rho_{s,in}$ is proportional to the relative noise in the penetration depth data. That implies a larger noise for smaller values of $\lambda_{in}(0)$, which becomes substantial for $\lambda_{in}(0)$ of the order of 1 μm. Finally, we point out that the shapes of curves for the in-plane and out-of-plane penetration depths in the ground state are qualitatively different from the s-wave dependence.

The behavior for the in-plane $\rho_{s,in}$ and out-of-plane $\rho_{s,out}$ superfluid densities for the intermediate state of sample S2 (established in the R state) is displayed in Fig. 9. Here, $\rho_{s,in}$ data are insensitive to the systematic error at low temperatures, since the correction for λ_{in} drops out from the expression for $\rho_{s,in}$. Note that the leading term, describing the low-

FIG. 7. Sample S1: (a) in-plane and (b) out-of-plane superfluid densities for the ground (R) state. Solid line is a fit to the polinomial expression. A large noise in $\rho_{s,in}$ is due to small values of $\lambda_{in}(0)$ (see text).
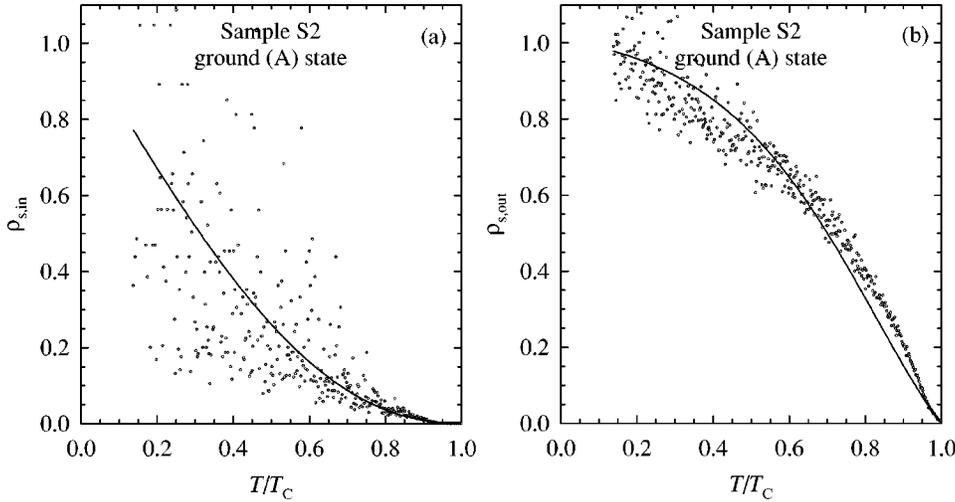
FIG. 8. Sample S2: (a) in-plane and (b) out-of-plane super-fluid densities for the ground (*A*) state. Solid line is a fit to the poli-nomial expression. A large noise in $\rho_{s,in}$ is due to small values of $\lambda_{in}(0)$ (see text).

temperature behavior, is the T^2 term for both the in-plane and out-of-plane superfluid densities:

$$\rho_{s,in} = 1 - 1.69t^2 + 2.77t^3 - 5.05t^4 + 2.97t^5, \qquad (16)$$

$$\rho_{s,out} = 1 - 1.02t^2 + 1.34t^3 - 2.50t^4 + 1.18t^5. \qquad (17)$$

In order to demonstrate the fact that the superfluid density behavior in the intermediate state is also rather close to the dependence expected for the *s*-wave order parameter behavior, the *s*-wave model dependence is added as a dashed line for both orientations.

IV. DISCUSSION

We start the discussion by pointing out that the well-defined, ground-state properties—complex susceptibility, penetration depth, and superfluid density—were essentially reproducible for all studied single crystals from both syntheses S1 and S2. Cooling-rate-dependent effects were also reproducible, but the observed behavior was the same only for single crystals from the same synthesis, while it differed significantly from the observed behavior for single crystals from the other synthesis.

First, we would like to comment on the anisotropy in T_C.

As in the previously published paper,[15] we have established that $\Delta T_C = 0.5$ K for $H_{ac}\perp$ and $H_{ac}\parallel$ plane geometry cannot be ascribed to the experimental error. We suggest that this anisotropy might be the consequence of the fact that the diamagnetic shielding is no longer effective for $H_{ac}\parallel$ plane geometry in the range of 0.5 K below T_C, which is due to the small sample dimensions and huge out-of-plane (Josephson-like) penetration depth near T_C. However, we point out that the T_C anisotropy has negligible effects, if any, on our data analysis, which is primarily done in the low-temperature region and therefore does not influence the resulting conclusions.

Second, we address the observed differences in cooling rate effects between samples S1 and S2. As pointed out earlier, both samples show the same behavior in the ground state: almost full diamagnetism for $H_{ac}\perp$ plane and the same temperature dependence and zero-temperature value of the in-plane and the out-of-plane penetration depths, as well as the same superfluid density temperature dependence. However, we note that sample S2 required a completely different cooling procedure with significantly longer time spent in the temperature region around 80 K, compared to sample S1, in order to accomplish the ground state. Moreover, sample S2 is much less sensitive to the cooling rate. That is, the difference
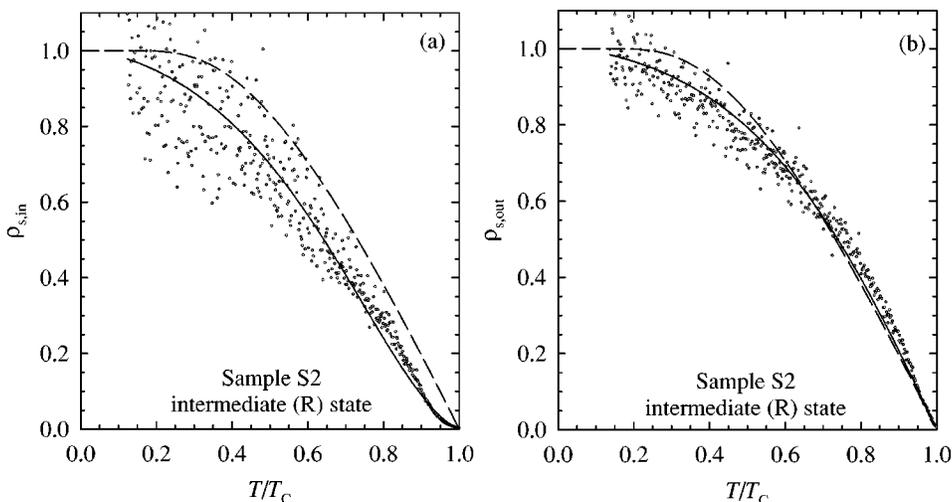
FIG. 9. Sample S2: (a) in-plane and (b) out-of-plane super-fluid densities for the intermediate (*R*) state. Solid line is a fit to the polinomial expression, and dashed line presents the *s*-wave model (see text).

regarding low-temperature susceptibility and zero-temperature penetration depth values between A and Q states for sample S2 is much smaller than the difference between R and Q states for sample S1. Both features indicate that (i) the low-temperature state is critically determined by the time scale of experiment in the region of glass transition and (ii) relaxation times of ethylene groups in the single crystals originating from synthesis S2 are much longer than the ones in the single crystals originating from synthesis S1. When the applied time scale is much longer than the relaxation time of the ethylene moieties, the low-temperature state is the ground state. In contrast, if the relaxation time exceeds the time scale of experiment, remnant disorder at low temperatures will be substantial and the Q state will be established. Different relaxation times of ethylene groups might also explain why the resistivity ratio RR(75 K/T_{min}) is much larger for samples from synthesis S1 when a standard slow cooling rate is applied. At this stage, we can only speculate about the possible origin of different relaxation times. The experimental observations that the crystals from synthesis S2 show weak metallic behavior, instead of a semiconducting behavior between RT and 100 K observed for samples of synthesis S1, might be of the same origin. Since the RT resistivity values do not differ substantially, we propose that subtle local variations of the impurity level in nominally pure samples from different syntheses might be responsible for the observed differences.

Next we comment on the behavior of the in-plane superfluid density in the ground state. The temperature dependence of the in-plane superfluid density for the d-wave superconducting order parameter $\Delta(\vec{k}) = \Delta \cos(2\phi)$, where ϕ is the angle between the quasiparticle momentum $\vec{k}$ and the $\vec{a}$ axis, within the weak-coupling theory, is given by[15,47]

$$\rho_{s,in}(t) \approx 1 - 0.6478t - 0.276t^3. \tag{18}$$

The coefficient a of the leading term t in $\rho_{s,in} = 1 - at + \cdots$ depends strongly on the ratio of the superconducting transition temperature and the zero-temperature superconducting order parameter. A comparison of values for a in Eq. (18) to those in Eqs. (12) and (14) suggests that the superconducting order parameter at $T = 0$ K is much smaller than that predicted by the weak-coupling limit. As a result, this would also imply that the nodal region, which volume is inversely proportional to the angular slope of the gap near the node[48] $\mu = 1/\Delta \, d\Delta(\phi)/d\phi|_{node}$, occupies a much larger fraction of the phase space at low temperatures. We point out that we have reached the same conclusion already on the basis of previously obtained results.[15] In the latter case, we did not evaluate $\lambda_{in}(0)$ from our measurements, but rather we used the values reported in the literature. Following the same procedure as in Ref. 15, we can again use uncalibrated data from present measurements and calculate the deviation of λ_{in} from the minimum value at the lowest attainable temperature $\lambda_{in}(T) - \lambda_{in}(T_{min})$.[15] Then, if we take the penetration depth value at 0 K given in the literature,[23,44–46] $\lambda_{in}(0) \approx 1$ μm, we get the same result; that is, the leading coefficient is much larger than expected in the weak-coupling model. In addition, we point out that the same behavior of ρ_{in} for
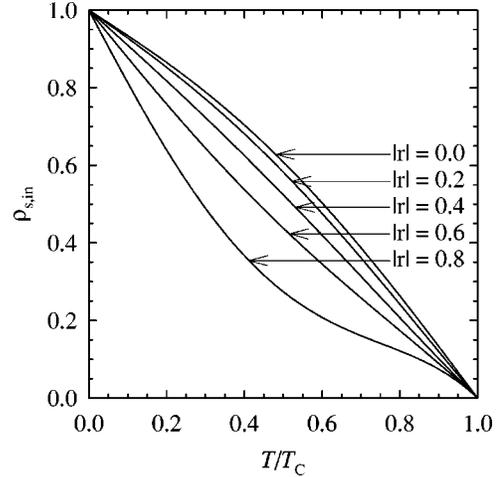
FIG. 10. Superfluid density in the $(d+s)$-wave model for a few values of the s-wave component parameter r.

$\lambda_{in}(0) \lesssim 1.3$ μm was reported by Carrington et al.[14] They pointed out that only at $\lambda_{in}(0) \gtrsim 1.8$ μm does the slope become similar to the one reported for high-T_C cuprate superconductors and expected in the weak-coupling model. From our present data, we get $\lambda_{in}(0) \approx 3$ μm for the crossover in-plane penetration depth value. One possibility to interpret our results is to consider the mixture of d-wave and s-wave order parameters, which corresponds to the superconducting order parameter $\Delta(\vec{k}) = \Delta[\cos(2\phi) + r]$, with r representing the s-wave component.[49] In this case the leading linear coefficient a increases with the increase of r according to the expression

$$a = \frac{2 \ln 2}{2.14\sqrt{1-r^2}} \exp\left[\frac{2r^2}{1+2r^2}\right]. \tag{19}$$

The shapes of the superfluid density curves for several values of parameter r are given in Fig. 10. For our results, $|r| \approx 0.7$ gives a very good agreement, which is, on the other hand, theoretically very unlikely. Recently, an admixture of the s-wave component with $r = -0.067$ for κ-(BEDT-TTF)Cu(NCS)$_2$ was suggested[49] from analysis of the angular-dependent magnetothermal conductivity data.[18] These data suggest that $d_{x^2-y^2}$-wave instead of d_{xy}-wave pairing is responsible for the superconductivity in κ-(ET)$_2$X materials. This implies that both Fermi surfaces participate in pairing in contrast to previous assumptions.[50] Since in the former case the spin fluctuation model for the κ-(ET)$_2$X materials no longer describes the superconductivity pairing, the origin should be found elsewhere. A coulomb interaction, which is responsible for the d-wave superconductivity, gives rise to both spin and charge fluctuations, so the obvious solution appears to be that charge fluctuations play the principal role in the κ-(ET)$_2$X superconductivity. The value $r = -0.07$ suggests that the nodal lines in $\Delta(\vec{k})$ pass through the gap between two Fermi surfaces. This is consistent with the $(d+s)$-wave model in which the superconductivity is due to charge fluctuations between different groups of dimers. On the other hand, for $r \approx -0.7$, the nodal directions cross the

2D circular Fermi surface, and for $r \approx 0.7$, the nodal directions cross the 1D Fermi surface. If the $d+s$ superconductivity model is generated by charge fluctuations, such a scenario is unlikely to work, since this implies a strong intra-Coulomb repulsion in each energy band.

Now, we address the behavior of the in-plane superfluid density in the intermediate state (Fig. 9). Considering the polynomial fit in Eq. (16), we see that the in-plane superfluid density appears to fit very well the d-wave model with impurity scattering in the unitary limit.[51–53] However, there is a serious discrepancy between our experimental data and the impurity model. First of all, we ascribe the difference between the A state (ground state), R state (intermediate state), and Q state to the residual degree of the ethylene disorder. The annealed state we discussed is the ground state with the least disorder in the ethylene groups. It is natural to assume that the ethylene disorder gives rise to the quasiparticle scattering, which changes the t-linear dependence of $\rho_{s,in}$ into the t-squared dependence. But this is in contradiction with the well-established fact that a small disorder depresses T_C dramatically.[51,52] In our experiment, it seems that T_C is practically unaffected by the ethylene disorder for the intermediate state, achieved by a slow cooling of -0.2 K/min in the region of the glass transition. Further, taking into account the fact that the $\lambda(0)$ increases for at least by a factor of 6, the superconducting electron density at 0 K, $n_s(0) \propto \lambda^{-2}(0)$, decreases at least by a factor of 36. A simple impurity model cannot describe the surprising combination of these two features. On the other hand, the results for other low-temperature states achieved by cooling rates $q_C < -1$ K/min for sample S1 and for the Q state in sample S2 are more consistent with the theory. In these cases both T_C, $\chi'(0)$, and therefore $\lambda(0)$ are concomitantly influenced by the remnant ethylene disorder. However, it is still difficult to correlate the observed behavior to the impurity model quantitatively. This discrepancy might indicate that the degree of disorder at low temperatures, as defined by the cooling rate in the region of the glass transition, has also a profound influence on electronic correlations, responsible for SC pairing. At this point we would like to recall the result of Kund *et al.*[30] showing changes in the crystal structure parameters in the region of the glass transition. It might be that these changes are also susceptible to the cooling rate. In addition, the authors of Ref. 6 have pointed out that the role of disorder in this class of superconductors might be different than in the other unconventional superconductors due to the vicinity of the Mott insulator in the phase diagram.

Coming back to the intermediate state, we suggest that the indication of the decrease in the superconducting electron density may be related to the reduction of the superconductivity volume. It has been already reported that cooling rates combined by progressive deuteration influence the low-temperature electronic state in κ-(ET)$_2$Br samples.[54,6] The deuterated κ-(ET)$_2$Br system is situated in the critical region between an insulating AF transition at 15 K and a SC transition at 11.5 K. Despite the slow cooling rate, the deuterated sample gives almost the same T_C as in the hydrogenated κ-(ET)$_2$Br system, the SC state being not fully established in the bulk. Note that this result strongly resembles what we

observed for S2 samples in the intermediate (R) state. In addition, a gradual decrease of the susceptibility below T_C in the deuterated system strongly indicates the inhomogenous nature of the SC state. This is in contrast to what we observe in sample S2, in which the susceptibility curves are rather sharp even in the Q state. More rapid cooling rates induce a decrease of T_C and a substantial decrease of the SC volume fraction. The authors of Refs. 54 and 6 have argued that since the electronic specific heat of rapidly cooled deuterated samples did not show any finite electronic contribution at low temperatures, the missing part of the superconducting phase should be considered to be the magnetic insulating phase. The question arises if their conclusion might also be valid in the hydrogenated system. Taking into account the structure of the phase diagram of this class of superconductors,[5] we think that this might be the case. However, specific heat data under carefully controlled cooling cycles are needed to resolve this issue.

The most intriguing fact about Fig. 9 is that in the intermediate state the observed data could be well described by the s-wave model as well. This gives a possible explanation for the contradictory findings in favor of the s-wave and d-wave models in the same material. The behavior is obviously strongly influenced by both thermal history and synthesis, which suggests that the same material was not measured in the same low-temperature state. We hope that our results could contribute to reconcile contradictory findings met in the past.

V. CONCLUSION

The level of residual disorder and the electronic properties at low temperatures are critically determined by the time scale of the experiment in the region of the glassy transition and the sample synthesis. This fact imposes an additional requirement to get a reliable description of the SC state and that is to perform a full characterization of the SC state in the sample under study in the same well-defined and -controlled cooling conditions. The origin of the observed differences can be attributed to the residual ethylene disorder, which might be theoretically considered as the impurity effect.

The in-plane superfluid density of the ground state with the lowest residual ethylene disorder exhibits clear T-linear dependence, which is consistent with the d-wave model and in contradiction with the s-wave model. The leading T-linear coefficient is much larger than the one expected for the weak-coupling d-wave model. The $(d+s)$-wave model can remove this numerical discrepancy. However, the rather large s-wave component needed to fit our data is not consistent with the recent thermal conductivity results.

On the other hand, the in-plane superfluid density of the intermediate state achieved by the slow cooling of -0.2 K/min in samples of one synthesis, as well as in the states achieved by rapid cooling rates ($q_C < -1$ K/min) in all studied samples, clearly exhibits the T-squared dependence, consistent with d-wave superconductivity in the presence of impurities. In the intermediate state, the same T_C as in the ground state is accompanied by a relatively large reduction in the superconducting electron density, which can-

not be explained within the standard impurity model. In the rapidly cooled states, T_C does reduce concomitantly with $\lambda(0)$; still the depression of T_C is quantitatively too small and the reduction of the superconducting electron density is too large. More work, both theoretical and experimental, is needed to resolve these issues.

Finally, the in-plane superfluid density data in the intermediate state can be relatively well fitted to the s-wave model data as well. This fact gives a possible explanation for the contradictory findings in favor of s-wave and d-wave models in the same material and will hopefully contribute to

a long awaited consensus regarding the pairing symmetry in the κ-(BEDT-TTF)-based superconductors. In this circumstance, specific heat measurements in the same well-defined and -controlled cooling conditions are highly desirable.

*Electronic address: mpinter@ifs.hr

[1] H. Urayama, H. Yamochi, G. Saito, K. Nozawa, T. Sugano, M. Kinoshita, S. Sato, K. Oshima, A. Kawamoto, and J. Tanaka, Chem. Lett. **1988**, 55 (1988).

[2] A.M. Kini, U. Geiser, H.H. Wang, K.D. Carlson, J.M. Williams, W.K. Kwok, K.G. Vandervoort, J.E. Thompson, D.L. Stupka, D. Jung, and M.-H. Whangbo, Inorg. Chem. **29**, 2555 (1990).

[3] M. Pinterić, M. Miljak, N. Biškup, O. Milat, I. Aviani, S. Tomić, D. Schweitzer, W. Strunz, and I. Heinen, Eur. Phys. J. B **11**, 217 (1999).

[4] K. Miyagawa, A. Kawamoto, Y. Nakazawa, and K. Kanoda, Phys. Rev. Lett. **75**, 1174 (1995).

[5] S. Lefebvre, P. Wzietek, S. Brown, C. Bourbonnais, D. Jérome, C. Mézière, M. Fourmigué, and P. Batail, Phys. Rev. Lett. **85**, 5420 (2000).

[6] H. Taniguchi, A. Kawamoto, and K. Kanoda, Phys. Rev. B **59**, 8424 (1999).

[7] P. Wzietek, H. Mayaffre, D. Jérome, and S. Brazovskii, J. Phys. I **6**, 2011 (1996).

[8] T. Arai, K. Ichimura, K. Nomura, S. Takasaki, J. Yamada, S. Nakatsuji, and H. Anzai, Synth. Met. **120**, 707 (2001).

[9] H. Mayaffre, P. Wzietek, D. Jérome, C. Lenoir, and P. Batail, Phys. Rev. Lett. **75**, 4122 (1995).

[10] Y. Nakazawa and K. Kanoda, Phys. Rev. B **55**, R8670 (1997).

[11] S. Belin, K. Behnia, and A. Deluzet, Phys. Rev. Lett. **81**, 4728 (1998).

[12] D. Achkir, M. Poirier, C. Bourbonnais, G. Quirion, C. Lenoir, P. Batail, and D. Jérome, Phys. Rev. B **47**, 11 595 (1993).

[13] L.P. Le *et al.*, Phys. Rev. Lett. **68**, 1923 (1992).

[14] A. Carrington, I.J. Bonalde, R. Prozorov, R.W. Giannetta, A.M. Kini, J. Schlueter, H.H. Wang, U. Geiser, and J.M. Williams, Phys. Rev. Lett. **83**, 4172 (1999).

[15] M. Pinterić, S. Tomić, M. Prester, D. Drobac, O. Milat, K. Maki, D. Schweitzer, I. Heinen, and W. Strunz, Phys. Rev. B **61**, 7033 (2000).

[16] K. Kanoda, K. Akiba, K. Suzuki, T. Takahashi, and G. Saito, Phys. Rev. Lett. **65**, 1271 (1990).

[17] T. Arai, K. Ichimura, K. Nomura, S. Takasaki, J. Yamada, S. Nakatsuji, and H. Anzai, Phys. Rev. B **63**, 104518 (2001).

[18] K. Izawa, H. Yamaguchi, T. Sasaki, and Y. Matsuda, Phys. Rev. Lett. **88**, 027002 (2002).

[19] Y.-N. Xu, W.Y. Ching, Y.C. Jean, and Y. Lou, Phys. Rev. B **52**, 12 946 (1995).

[20] R. Louati, S. Charfi-Kaddour, A. Ben Ali, R. Bennaceur, and M. Héritier, Phys. Rev. B **62**, 5957 (2000).

[21] D.R. Harshman, R.N. Kleiman, R.C. Haddon, S.V. Chichester-Hicks, M.L. Kaplan, L.W. Rupp, Jr., T. Pfiz, D.L. Williams, and D.B. Mitzi, Phys. Rev. Lett. **64**, 1293 (1990).

[22] M. Lang, N. Toyota, T. Sasaki, and H. Sato, Phys. Rev. Lett. **69**, 1443 (1992).

[23] M. Dressel, O. Klein, G. Grüner, K.D. Carlson, H.H. Wang, and J.M. Williams, Phys. Rev. B **50**, 13 603 (1994).

[24] H. Elsinger, J. Wosnitza, S. Wanka, J. Hagel, D. Schweitzer, and W. Strunz, Phys. Rev. Lett. **84**, 6098 (2000).

[25] J. Müller, M. Lang, R. Helfrich, F. Steglich, and T. Sasaki, Phys. Rev. B **65**, 140509 (2002).

[26] S.L. Lee, F.L. Pratt, S.J. Blundell, C.M. Aegerter, P.A. Pattenden, K.H. Chow, E.M. Forgan, T. Sasaki, W. Hayes, and H. Keller, Phys. Rev. Lett. **79**, 1563 (1997).

[27] H. Akutsu, K. Saito, and M. Sorai, Phys. Rev. B **61**, 4346 (2000).

[28] J. Müller, M. Lang, F. Steglich, J.A. Schlueter, A.M. Kini, and T. Sasaki, Phys. Rev. B **65**, 144521 (2002).

[29] U. Geiser, A.J. Schultz, H.H. Wang, D.M. Watkins, D.L. Stupka, J.M. Williams, J.E. Schirber, D.L. Overmyer, D. Jung, J.J. Novoa, and M.-H. Whangbo, Physica C **174**, 475 (1991).

[30] M. Kund, H. Müller, W. Biberacher, K. Andres, and G. Saito, Physica B **191**, 274 (1993).

[31] Y. Watanabe, H. Sato, T. Sasaki, and N. Toyota, J. Phys. Soc. Jpn. **60**, 3608 (1991).

[32] X. Su, F. Zuo, J.A. Schlueter, M.E. Kelly, and J.M. Williams, Phys. Rev. B **57**, R14 056 (1998).

[33] L.I. Buravov, N.D. Kushch, V.A. Merzhanov, M.V. Osherov, A.G. Khomenko, and E.B. Yagubskii, J. Phys. I **2**, 1257 (1992).

[34] D. Schweitzer and M. Schiller (unpublished).

[35] L.K. Montgomery, R.M. Vestal, K.P. Starkey, B.W. Fravel, M.J. Samide, D.G. Peters, C.H. Mielke, and J.D. Thompson, Synth. Met. **103**, 1878 (1999).

[36] C.H. Mielke, N. Harrison, D.G. Rickel, A.H. Lacerda, R.M. Vestal, and L.K. Montgomery, Phys. Rev. B **56**, R4309 (1997).

[37] H. Taniguchi and K. Kanoda, Synth. Met. **103**, 1967 (1999).

[38] S. Tomić, M. Pinterić, M. Prester, D. Drobac, and K. Maki, Physica C **364-365**, 247 (2001).

[39] http://www.cryobind.com/.

[40] J. Hagel, S. Wanka, D. Beckmann, J. Wosnitza, D. Schweitzer, W. Strunz, and M. Thumfart, Physica C **291**, 213 (1997).

[41] D. Drobac, J. Magn. Magn. Mater. **183**, 71 (1998).

[42] G.W. Crabtree, Phys. Rev. B **16**, 1117 (1977).

[43] K. Kanoda (unpublished).

[44] P.A. Mansky, P.M. Chaikin, and R.C. Haddon, Phys. Rev. B **50**, 15 929 (1994).

[45] N.H. Tea, F.A.B. Chaves, U. Klostermann, R. Giannetta, M.B.

Salamon, J.M. Williams, H.H. Wang, and U. Geiser, Physica C **280**, 281 (1997).

[46] M. Lang, Supercond. Rev. **2**, 1 (1996).

[47] H. Won and K. Maki, Phys. Rev. B **49**, 1397 (1994).

[48] D. Xu, S.K. Yip, and J.A. Sauls, Phys. Rev. B **51**, 16 233 (1995).

[49] H. Won and K. Maki, Physica B **312-313**, 44 (2002).

[50] R. Louati, S. Charfi-Kaddour, A. Ben Ali, R. Bennaceur, and M. Héritier, Synth. Met. **103**, 1857 (1999).

[51] Y. Sun and K. Maki, Phys. Rev. B **51**, 6059 (1995).

[52] Y. Sun and K. Maki, Europhys. Lett. **32**, 355 (1995).

[53] P.J. Hirschfeld and N. Goldenfeld, Phys. Rev. B **48**, 4219 (1993).

[54] A. Kawamoto, K. Miyagawa, and K. Kanoda, Phys. Rev. B **55**, 14 140 (1997).

[55] M. Tinkham, *Introduction to Superconductivity* (McGraw-Hill, New York, 1996), p. 25.

[56] This state should not, by any means, be identified with the historical notion of the intermediate state in superconductors (Ref. 55).